EXOSKELETONS

OpenExo: An open-source modular exoskeleton to augment human function

Jack R. Williams[1]*, Chance F. Cuddeback[1], Shanpu Fang[1], Daniel Colley[1], Noah Enlow[1], Payton Cox[2], Paul Pridham[3], Zachary F. Lerner[1,4]*

Although the field of wearable robotic exoskeletons is rapidly expanding, there are several barriers to entry that discourage many from pursuing research in this area, ultimately hindering growth. Chief among these is the lengthy and costly development process to get an exoskeleton from conception to implementation and the necessity for a broad set of expertise. In addition, many exoskeletons are designed for a specific utility and are confined to the laboratory environment, limiting the flexibility of the designed system to adapt to answer new questions and explore new domains. To address these barriers, we present OpenExo, an open-source modular untethered exoskeleton framework that provides access to all aspects of the design process, including software, electronics, hardware, and control schemes. To demonstrate the utility of this exoskeleton framework, we performed benchtop and experimental validation testing with the system across multiple configurations, including hip-only incline assistance, ankle-only indoor and outdoor assistance, hip-and-ankle load carriage assistance, and elbow-only weightlifting assistance. All aspects of the software architecture, electrical components, hip and Bowden-cable transmission designs, and control schemes are freely available for other researchers to access, use, and modify when looking to address research questions in the field of wearable exoskeletons. Our hope is that OpenExo will accelerate the development and testing of new exoskeleton designs and control schemes while simultaneously encouraging others, including those who would have been turned away from entering the field, to explore new and unique research questions.

INTRODUCTION

Exoskeletons hold potential as mobility-enhancing and rehabilitative tools capable of transforming how, when, and where individuals engage in activity. Although the field is relatively young, it has seen a substantial increase in interest within the past 15 years. Termed "the exoskeleton expansion" by Sawicki and colleagues (*1*), this increased interest has led to the development of tools with a wide range of applications, including rehabilitative devices to aid those with movement deficits [such as individuals with cerebral palsy (*2*–*4*), stroke (*5*–*8*), or age-related mobility limitations (*9*–*11*)], assistive devices to enhance mobility across varied activities (*12*–*14*), military devices to amplify soldiers' ability (*15*, *16*), and ergonomic devices to increase productivity and/or minimize injury in demanding workplace environments (*17*–*19*).

Despite a large increase in activity within the field of wearable robotics, it is still in its relative infancy. One reason for this continued infancy is the field's considerable barrier to entry. This barrier is characterized by a lengthy and costly developmental process that involves designing software, electronics, hardware, and control schemes. Each of these stages is independently challenging and often interconnected, leading to a multistep, iterative process that requires a substantial investment of time and resources before original research can be performed. An additional barrier is that the field is relatively inaccessible to nonexperts. That is, to develop an exoskeleton device, one needs expertise in a broad set of domains, including mechanical and electrical engineering, robotics and controls, and biomechanics, which can be prohibitive for those lacking experience in one of these disciplines (such as biomechanists). In addition to a high barrier to entry, the field is also limited by the use of highly specialized, organizationally embedded systems. This limitation manifests in several different ways. First, the creation of highly specialized devices (such as a device solely focused on ankle plantar flexion) leads to inefficiencies when researchers want to explore a new domain (like the hip joint) because much of the software and hardware used in one device will have to be adapted to interface with a new device. Second, there is a large variety of organization-specific software and hardware that groups use to conduct their research. This results in increasingly isolated and specialized systems that make research harder to replicate, further contributing to the reproducibility crisis faced by much of the research community (*20*). Last, these specialized, closed-source devices typically lead to small sample sizes during experimental testing, which increases the likelihood of irreproducible work. One solution to these challenges would be the establishment of a fully open-source exoskeleton system. Similar devices in other fields, such as prosthetics (*21*) and quadrotor flight (*22*), have proven to be valuable tools to new and established researchers. Some have tried to develop open-source exoskeleton devices before, such as OpenBionics' exoskeleton glove (*23*), flexible, scalable electronics architecture (FlexSEA) (*24*), and the pediatric-focused assistive lower limb controlled exoskeleton (*25*), but these devices are highly specialized and thus relatively inflexible and therefore less likely to be adopted. These challenges could be addressed by developing a fully open-source system that is accessible to those without complete expertise in the field while simultaneously being flexible enough to facilitate new device designs with minimal changes needed to the system's architecture.

To address this, we have created OpenExo, a modular open-source exoskeleton system (software, hardware, electronics, and controls) for researchers and curious global citizens to access, use, and expand

[1]Department of Mechanical Engineering, Northern Arizona University, Flagstaff, AZ, USA. [2]School of Informatics, Computing, and Cyber Systems, Northern Arizona University, Flagstaff, AZ, USA. [3]Department of Industrial and Operations Engineering, University of Michigan, Ann Arbor, MI, USA. [4]College of Medicine–Phoenix, University of Arizona, Phoenix, AZ, USA.
*Corresponding author. Email: jack.williams@nau.edu (J.R.W.); zachary.lerner@nau.edu (Z.F.L.)

as they see fit. Here, we present the design of the software, electronics, and hardware interfaces of this open-source system, characterize its performance, and demonstrate its modularity by assessing functionality under a variety of assistive configurations (hip-only, ankle-only, hip-and-ankle, and elbow). Our hope is that our community and those who wish to enter the field will embrace OpenExo, use it to interface with original joint assembly end effectors, and bring us closer to making exoskeletons a reality of everyday life.

RESULTS

Open-source tool

All resources related to OpenExo (Fig. 1 and Movie 1) can be found at theopenexo.org. This includes a software package capable of use with or without modification to support the testing of new hardware and control approaches without the need for extensive development of supporting code (fig. S1); a detailed electrical architecture (fig. S2), including a printed circuit board (PCB) designed to interface with the software package while actuating up to four individual joints simultaneously; and an open-source hip design (fig. S3A) and Bowden-cable transmission system (figs. S3B and S4). These resources are supported with documentation to help facilitate usage and modification for experts and novices alike. This includes a guide to the structure and function of the software and how to perform key modifications, like adding new joints, controllers, sensors, and motors, and a guide to introduce novices to the programming language used throughout (C++). This also includes information on using a companion Python application capable of facilitating device operation while giving users the ability to modify control parameters and monitor/store data in real time. We have also detailed the structure and function of the PCB, included information on how and where to get it externally manufactured, and provided the files needed to enable researchers to modify it for their own needs. Last, we have provided supporting documentation for the construction of a direct-drive hip device and a Bowden-cable transmission system. This includes part files, a complete bill of materials, a step-by-step guide to manufacturing and constructing (machining and assembly of parts and creation of wires and cables), and directions to third-party resources for those who lack the means to manufacture the hardware in house.

Design goals

There were several design goals that went into the creation of this system. First, we wanted to create a device that could be used in any setting, including indoor, outdoor, and mixed-terrain environments. Second, the device needed to have a logical and easy-to-follow software

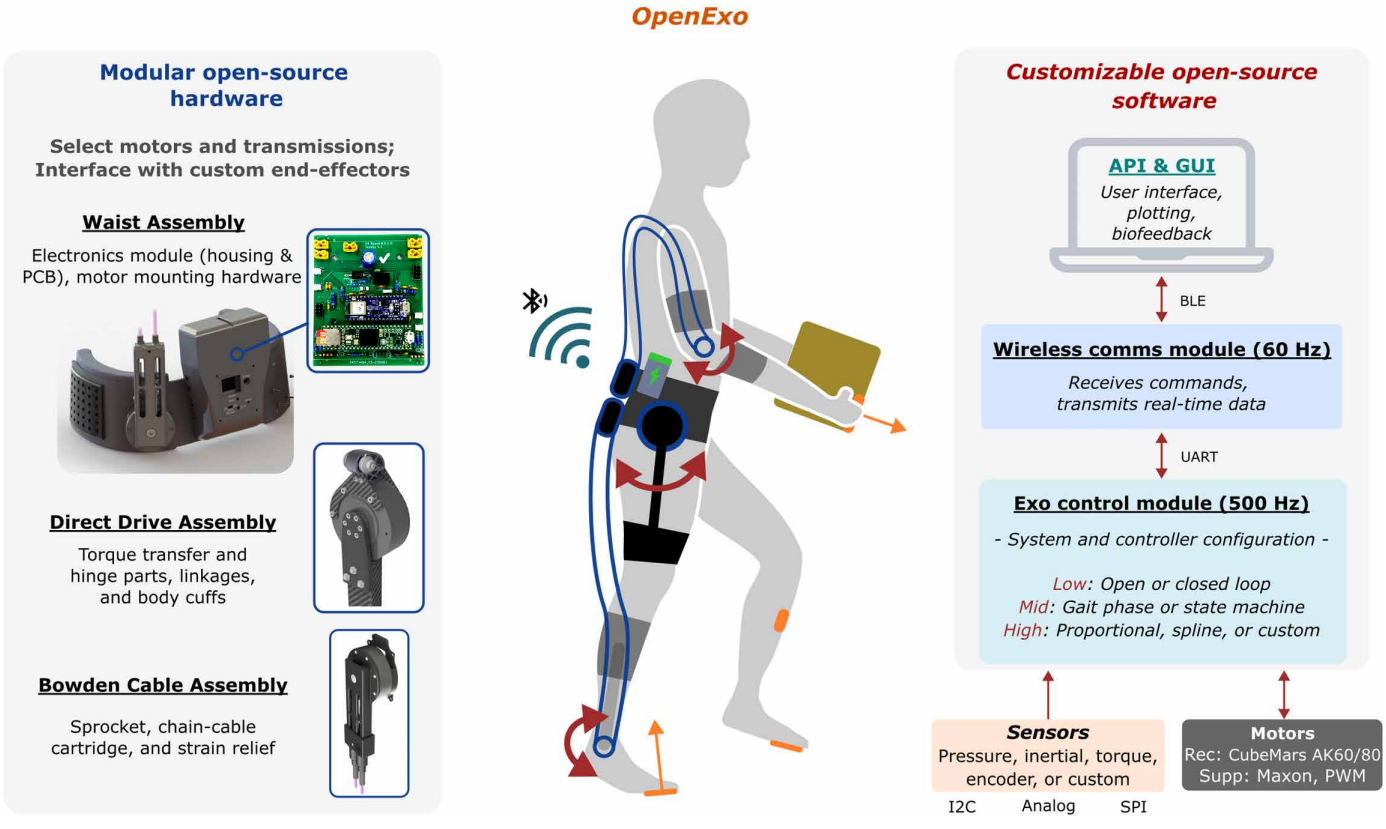

Fig. 1. Overview of OpenExo and its modular features, including swappable hardware components and customizable software. The modular hardware components include an untethered waist belt that houses the electronics and supports up to four motors at a time, with direct-drive and Bowden cable–based transmission options. The customizable software includes an open-source exoskeleton control package designed to have a high degree of modularity to accommodate new joints, motor types, sensors, and control approaches. This software also contains a companion Python application to help users operate and control the system in real time, including the ability to plot and store data, update controller parameters, and provide biofeedback. API, application programming interface; GUI, graphical user interface; BLE, bluetooth low energy; UART, universal asynchronous receiver-transmitter; PWM, pulse width modulation; I2C, interintegrated circuit; SPI, serial peripheral interface.

Movie 1. Overview of OpenExo, highlighting aspects of the software, electrical, and hardware components, as well as the benchtop engineering and experimental validation for the different configurations.

structure that would be accessible to both experts and novices. Third, we wanted a simple electrical architecture that could support both single- and multijoint applications while being easily revisable to meet researchers' needs. Fourth, we wanted a hardware system that could support multiple configurations, all of which could be easily swapped depending on the user's desired task. Fifth, we aimed to develop an easy-to-manufacture, low-cost hip configuration to enable novices to replicate our work and begin developing their own projects. Sixth, we sought to develop a Bowden-cable transmission system that could serve as a starting point for others to pursue innovative end-effector designs. Last, principles of modularity had to be embedded into all aspects of the system to facilitate testing of new hardware and control schemes without extensive modification. To summarize, we sought to design a single flexible system that could be customized to many different joint configurations while being capable of being used by anyone in any setting. To achieve this, we embedded principles of modularity in all components of the system including its software, electrical architecture, and hardware.

Software

The chief source of modularity in our system comes from the software architecture. Our software was developed using a combination of C++ and Arduino languages, with the principle of inheritance-based polymorphism (realized through parent-child and abstract classes) used to achieve a high-degree of modularity, reduce redundancy, and minimize dependencies. Figure S1 outlines the structure of the software, which was designed to have a logical, easy-to-follow form. The system starts broad and develops a narrower focus as it proceeds through its computations, starting with functions related to overall exoskeleton usage; accessing computations specific to each side; and then getting into computations specific to joints that include accessing the controllers, sensors, and motors assigned to those joints. The controller, sensor, and motor computations are all self-contained and accessed by instances of joints. That is, if you have a controller capable of operating on multiple joints, you do not need to repeat the controller definitions for each joint; they can be defined once and accessed by any joint that can operate the said controller.

To avoid having to directly modify the software every time a change in configuration was desired, we designed the system to pull in the configuration information from a file stored on a secure digital (SD) card. Through this, users can change which joints and sides of interest they would like to run as well as which controller is the default mode of operation for the specified joint. In addition, we developed a companion Bluetooth application in Python to allow users to update controller parameters and monitor and store data during operation.

Electrical architecture

Our focus was on developing simple, intuitive electronics to facilitate fabrication of an exoskeleton device among individuals who may not have expertise in electrical design. Previous open-source electrical architectures, such as FlexSEA (*24*), are extremely modular but also rather complex because of the use of multiple interconnected PCBs, which may limit more widespread adoption and discourage researchers from attempting revisions. We opted for a simpler approach that encourages iteration and revisability to help facilitate longer-term adoption.

Our PCB consists of one board that can support up to four individual joints at a time. We developed the board to interface with CubeMars' AK-series motors (Nanchang, China) because they are powerful enough to provide torques for larger adults and during more challenging tasks, such as multiterrain walking. In addition, there are multiple versions of these motors that all rely on the same communication scheme [controller area network (CAN)]. Thus, by designing the electronics and software to interface with CAN communication, researchers can choose which version of the AK-series motors to work with, further enhancing modularity. For example, if a researcher wanted to use the device on a pediatric individual or during a low-demand task, then the AK60-6v1.1 motor could be used because it has smaller torque-generating capabilities while being lighter than other versions. If a researcher wanted to use the device on an adult or during a higher-demand task, they could switch to the AK80-9 version to get higher torques at the trade-off of added mass. The board was also designed to take an eight-pin ribbon cable connector on each side, providing room for multiple analog sensor connections, such as force-sensitive resistors (FSRs) and torque transducers, that can aid in device control. Additional sensors and microcontrollers can be integrated with the electronics module using an interintegrated circuit, a serial peripheral interface, or further analog input/output breakout connections. Sensor data are collected and integrated with the control code at 500 Hz. Documentation on using differing communication protocols and for modifying the software to take new boards, sensors, and motor types is available to help users adapt the system to their needs.

Hardware

The software and electrical architectures were designed to be modular so that researchers could develop hardware capable of assisting

any upper- or lower-extremity joint of interest. To highlight this, we developed different configurations to interface with this system. This included hardware to aid the hip (fig. S3A), ankle (fig. S3B), and elbow (fig. S3D). All configurations were designed to interface with the same waist belt and can be combined (fig. S3) and swapped quickly (fig. S5) to enable researchers to explore new types of exoskeleton assistance with minimal retooling necessary (Fig. 2). To facilitate replication by nonexperts, the hip hardware was designed to be simple, easy to manufacture, low cost, and capable of operating accurately under open-loop control. In addition, we have included the design of our belt-side Bowden-cable transmission so that others may replicate and explore new end-effector design approaches via this form of actuation (fig. S4). In all cases, the hardware was designed to operate only with the electronics embedded in the waist belt to enable researchers to use the device in both indoor and outdoor settings.

Engineering validation

We quantified the capabilities of the system by completing benchtop and performance tests for each configuration. This included benchtop testing to characterize the responsiveness of the device to changes in torque, torque-tracking tests during functional operation to understand the accuracy of the prescribed assistance, duration testing to gain insight into the limiting factors surrounding device life span, and mechanical power characterization during functional operation (Supplementary Methods).

Benchtop testing

We characterized the responsiveness of each joint when subjected to a step response at experimentally relevant torque magnitudes (Fig. 3A). To achieve this, all devices needed an inline torque transducer so that applied torque could be measured and compared with what was prescribed. This required a small change in the design of the hip hardware (fig. S6A). In all cases, the device operated with the

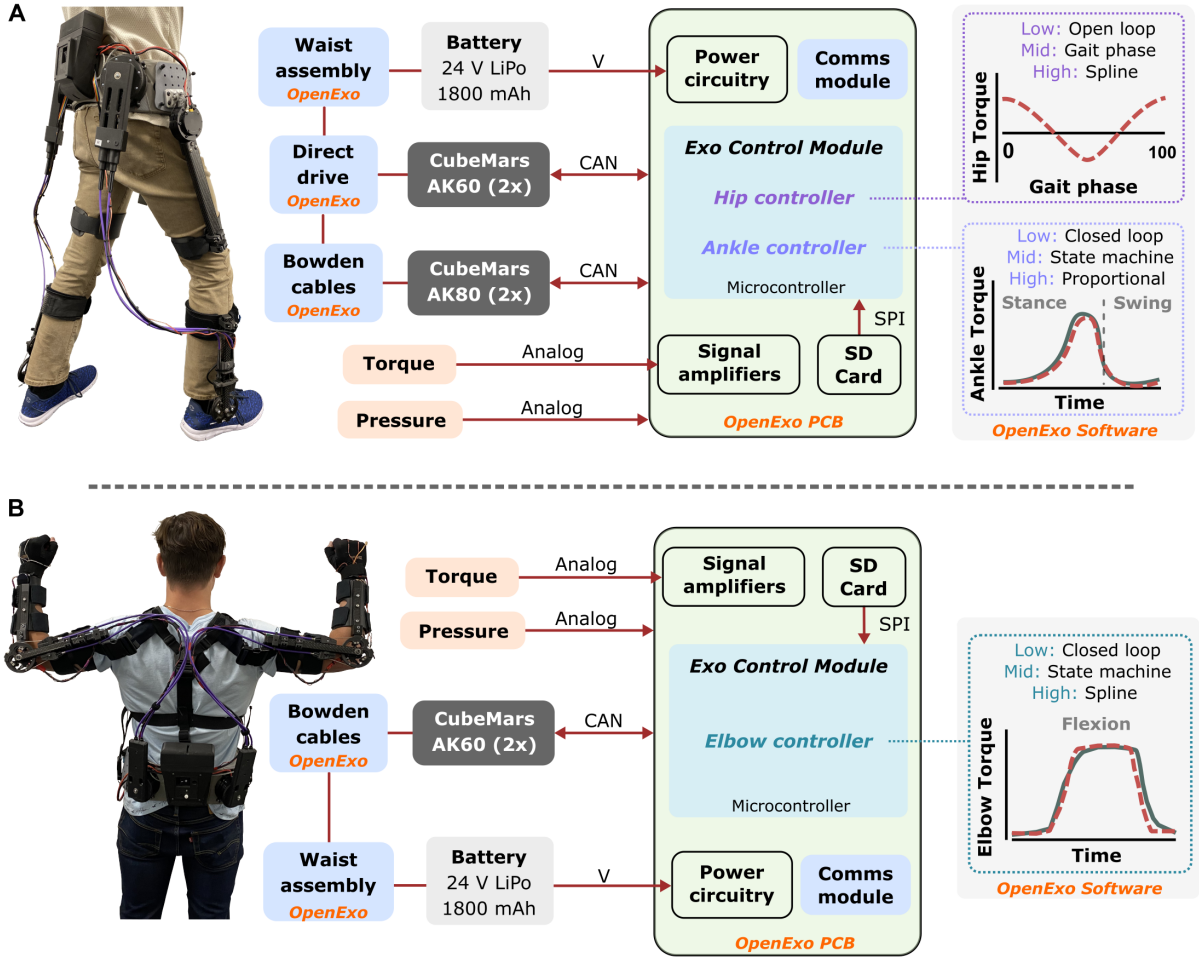

Fig. 2. OpenExo was designed to be modular to facilitate a variety of different configurations with minimal retooling. (**A**) Example hip-and-ankle configuration. Users can select different types of motors (AK60, AK70, or AK80) and different transmission systems (direct drive or Bowden cables) to facilitate joint actuation. These options interface with the PCB that also reads data from sensors, such as pressure sensors, to help facilitate control. A variety of low (closed- or open-loop), mid (gait phase or state machine), and high (spline based or proportional moment based) level control approaches is available. To enable seamless use without extensive retooling of the code, users can specify key configuration information (joints used, default controller/controller parameters, and sensors) on an SD card that interfaces with the PCB. Using the companion Python application, users can begin device operation, monitor sensor and exoskeleton data in real time, and update controllers and their parameters as needed. To switch to a different configuration, such as (**B**) an elbow-only configuration, all that users would need to do is switch out the hardware interfacing with the belt and modify the configuration information on the SD card. No modifications to the software or PCB are required. In each panel, the red dashed line represents prescribed torque, and the solid green line represents measured torque.

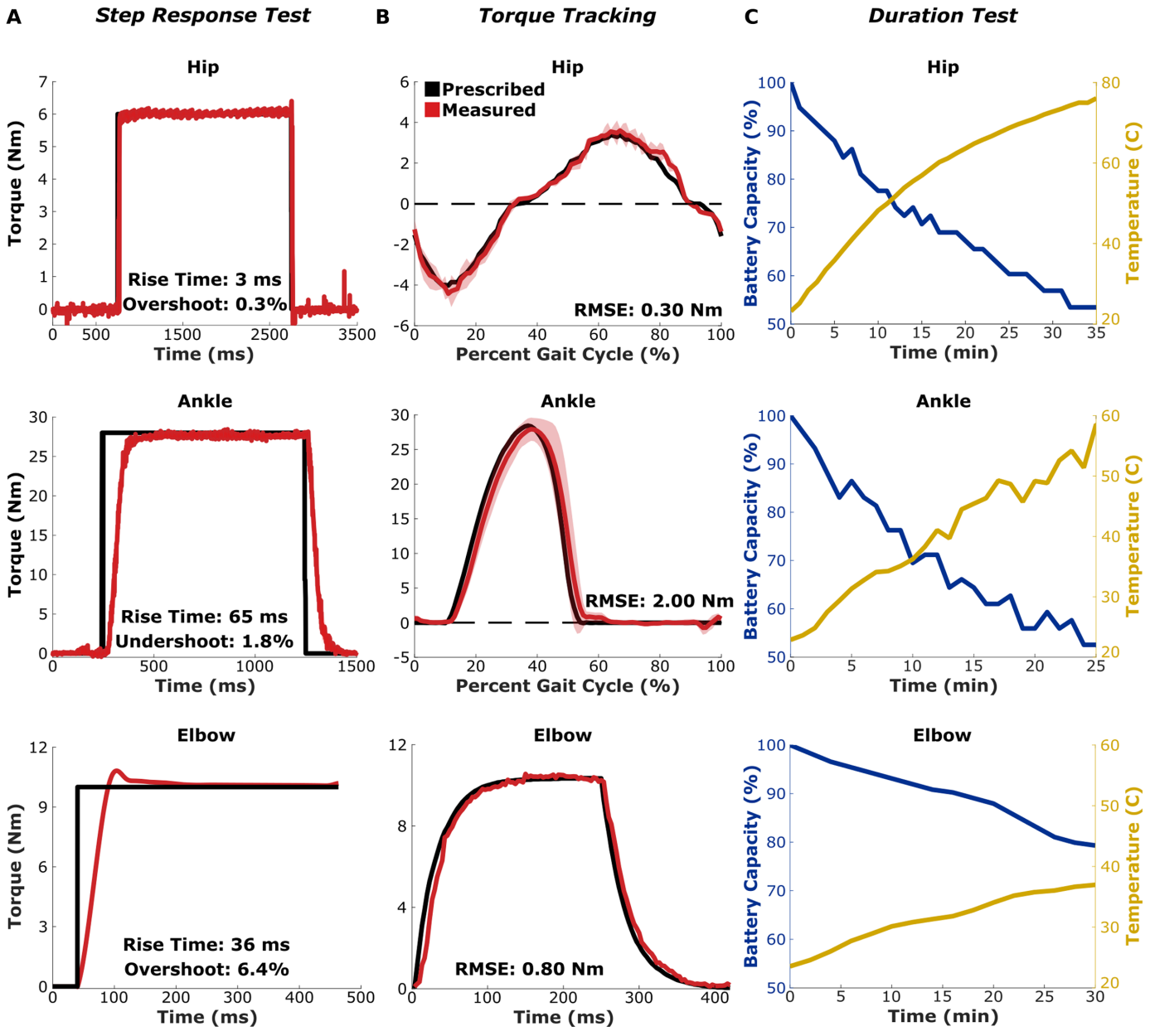

Fig. 3. Results from the benchtop validation and duration testing. (**A**) Step response test for the hip, ankle, and elbow configurations. Each configuration displayed fast rise times with minimal overshoot/undershoot. (**B**) Torque-tracking test for the hip, ankle, and elbow using the same control schemes as the experimental validation. Each configuration had a low tracking error (~7% of the maximum torque magnitude). The black line is the prescribed torque, and the red line is the average measured torque across all steps (for the hip and ankle configurations) or repetitions (for the elbow) from one user. The shaded regions represent 1 SD. (**C**) Battery capacity (blue) and motor temperature (gold) over the course of a duration test for the hip, ankle, and elbow configurations. The elbow configuration was halted after 30 min but had an estimated operation time of 72 min. In each case, the battery was the limiting factor. It should be noted that prolonged contact of skin (>5 s) on surfaces with temperatures exceeding 60°C may cause serious risk of injury, and we recommend incorporating heat shielding, available as an alternative hardware component (see documentation), into the design of each configuration as a precaution.

low-level control scheme intended for use while worn by a user. That is, the hip device, despite the presence of the torque transducer, operated under open-loop control, whereas the ankle and elbow devices operated under closed-loop control. When subjected to an open-loop step response of 6 Nm, the hip device had a rise time of 3.0 ms and an overshoot of 0.30%. During closed-loop control, the ankle configuration had a rise time of 65.0 ms and an undershoot of 1.8% when subjected to a step response of 28 Nm, whereas the elbow configuration had a rise time of 35.8 ms with an overshoot of 6.4% under a 10-Nm step response (*26*).

Torque tracking

To characterize the accuracy of the prescribed assistance, individuals donned and operated each configuration during its intended function while the measured and prescribed torques were recorded (Fig. 3B). While operating on a controller developed by Bryan *et al.* (*27*) and Franks *et al.* (*28*) and walking at a speed of 1.25 m s^{-1}, the

root mean square error (RMSE) of the hip device was 0.30 Nm (7.3% of the set point), suggesting that the control paradigm was accurate despite the lack of closed-loop control. While configured for ankle assistance using a previously described proportional joint moment controller (*29*, *30*) and walking at a speed of 1.25 m s^{-1}, the device maintained this same level of accuracy with a RMSE of 2.00 Nm (7.1% of the set point). Last, while assisting the user during a repetitive lifting task (*26*), the elbow configuration displayed a similar accuracy as the hip and the ankle, with a RMSE of 0.84 Nm (7.0% of the set point).

Duration testing

To fully characterize the utility of a device, it is important to understand how long it can operate and its limiting factors. Thus, a duration test was performed with a user operating the device in each configuration while using a 22.2-V, 1800-mAh lithium polymer (LiPo) battery (HRB; Fig. 3C). For the hip, ankle, and hip-and-ankle configurations, this involved walking on a treadmill at 1.25 m s^{-1} with hip flexion (5 Nm) and extension (5.5 Nm) assistance and/or ankle plantar flexion assistance (28 Nm). As the device operated under these conditions, the battery voltage and the motor temperatures were recorded at 1-min intervals. The test was halted once the motors reached their temperature limit (100°C) or the battery reached the manufacturer's recommended stopping voltage (3.7 V per cell = 22.2 V total). The room temperature for each test was 21.1°C. The open-loop hip configuration was able to operate for 35 min. During this time, the average motor temperature increased without reaching a steady state, whereas the battery voltage decreased steadily. At the end of the walk, the motors had reached a temperature of 76.7°C, whereas the battery had reached the manufacturer's recommended limit of 22.2 V (~900 mAh). The ankle configuration was able to operate for 25 min. Like the hip, the motor temperature continuously increased but failed to level off, reaching a temperature of 56.8°C, whereas the battery decreased until reaching the manufacturer's recommended limit. When configured to provide simultaneous assistance to the hip and ankle joints, the device was able to operate for 15 min. Like the other configurations, the motor temperatures failed to level off, reaching a temperature of 56.7°C at the hips and 40.8°C at the ankles, whereas the battery reached the manufacturer's limit (fig. S7). It should be noted that, although the manufacturer recommends a limit of 3.7 V per cell, this is with optimal long-term battery health in mind and likely represents a conservative estimate of battery life. For typical operation, it is likely that the battery could be operated down to ~3.2 V per cell (~19.2 V total) before reaching its true limit. As a result, the battery voltage is presented as a percentage capacity and is terminated at 50%.

To estimate the run time of the device when configured for elbow assistance, we had a user simulate a workplace task. Specifically, the individual lifted a 10-kg box off a table and carried it 10.8 m to a second table, where it was placed for 1 s before being lifted and carried 3.5 m back to the first table and placed in its original position (fig. S8). This cycle was repeated over a 30-min period while the user received 12 Nm of flexion assistance when holding the box. To simulate down time in a workplace environment, such as for product inspection, we had the user complete every third cycle without carrying the box. As the device operated under these conditions, the battery voltage and motor temperatures were recorded at 2-min intervals. After 30 min, the user had completed 122 cycles, and the device had reached 79% of its operating voltage (23.8 V) and capacity (1422 mAh) with a motor temperature of 37.6°C (Fig. 3C). Extrapolating this rate of power consumption, it would take ~72 min of operation or ~293 cycles until the battery reached the manufacturer's recommended limit (representing 50% of its capacity).

Experimental validation

To demonstrate the versatility and utility of our open-source system, we recruited healthy adults ($n = 7$; table S1) to complete activities while the device operated in its different configurations. We selected activities that we thought would elicit the most benefits from device usage. This included incline walking while configured for hip assistance ($n = 2$), because the hips contribute more to positive power generation during incline walking (*31*). This also included outdoor and indoor walking while configured for ankle assistance ($n = 1$), because the ankles contribute the most positive power during level walking (*31*). We sought a high-demand task for multijoint assistance and thus selected load carriage during level walking for the combined hip-and-ankle configuration ($n = 2$). Last, we had users lift weights to fatigue ($n = 2$) while the device was configured for elbow assistance.

Hip assistance during indoor incline walking

Two individuals (P1 and P2; table S1) performed incline treadmill walking trials at 7.5° while outfitted with a portable, indirect calorimetry metabolic unit (K5, COSMED). Both individuals walked at a comfortable walking speed (P1: 1.0 m s^{-1}; P2: 0.85 m s^{-1}) for 8 min with and without the device configured for hip assistance. Metabolic power for the last 2 min of each trial was calculated and normalized by body mass and walking speed to determine the steady-state cost of transport (COT) (*29*, *32*). Both participants displayed reductions in the COT while using the hip exoskeleton (versus without) during incline walking (Fig. 4A). P1 had an 8% reduction in COT (Shod: 6.72 J kg^{-1} m^{-1}; Exo: 6.17 J kg^{-1} m^{-1}) compared with the shod condition, whereas P2 had a 14% reduction (Shod: 7.35 J kg^{-1} m^{-1}; Exo: 6.29 J kg^{-1} m^{-1}).

Ankle assistance during level indoor treadmill walking

One individual (P3; table S1) completed metabolic testing trials with and without the device configured for ankle assistance during level indoor treadmill walking at a speed of 1.25 m s^{-1}. Each walking trial lasted 8 min, from which the COT during the last 2 min was used as a steady-state comparison between the conditions. The participant exhibited an 8% reduction in the COT while receiving ankle assistance compared with walking without the exoskeleton (Shod: 2.19 J kg^{-1} m^{-1}; Exo: 2.02 J kg^{-1} m^{-1}; Fig. 4B).

Hip-and-ankle assistance during walking with load carriage

Two individuals (P4 and P5; table S1) walked on a treadmill at a self-selected speed (P4: 1.25 m s^{-1}; P5: 1.25 m s^{-1}) while wearing a weighted vest with a moderately sized load (22.5% of body weight). Each user walked 8 min with and without the device configured for simultaneous hip-and-ankle assistance while metabolic data were collected via indirect calorimetry. The COT was calculated for the last 2 min of each condition to enable comparison between the approaches. Both participants had reductions in the COT with combined hip-and-ankle assistance (versus no device; Fig. 4C). P4 had an 8% reduction in the COT (Shod: 2.68 J kg^{-1} m^{-1}; Exo: 2.46 J kg^{-1} m^{-1}) compared with the shod condition, and P5 displayed an 18% reduction (Shod: 2.59 J kg^{-1} m^{-1}; Exo: 2.13 J kg^{-1} m^{-1}).

Ankle assistance during outdoor walking

To demonstrate the untethered nature of the system, the same individual who completed ankle-assisted indoor testing (P3; table S1) completed walking trials on outdoor terrain. This involved walking

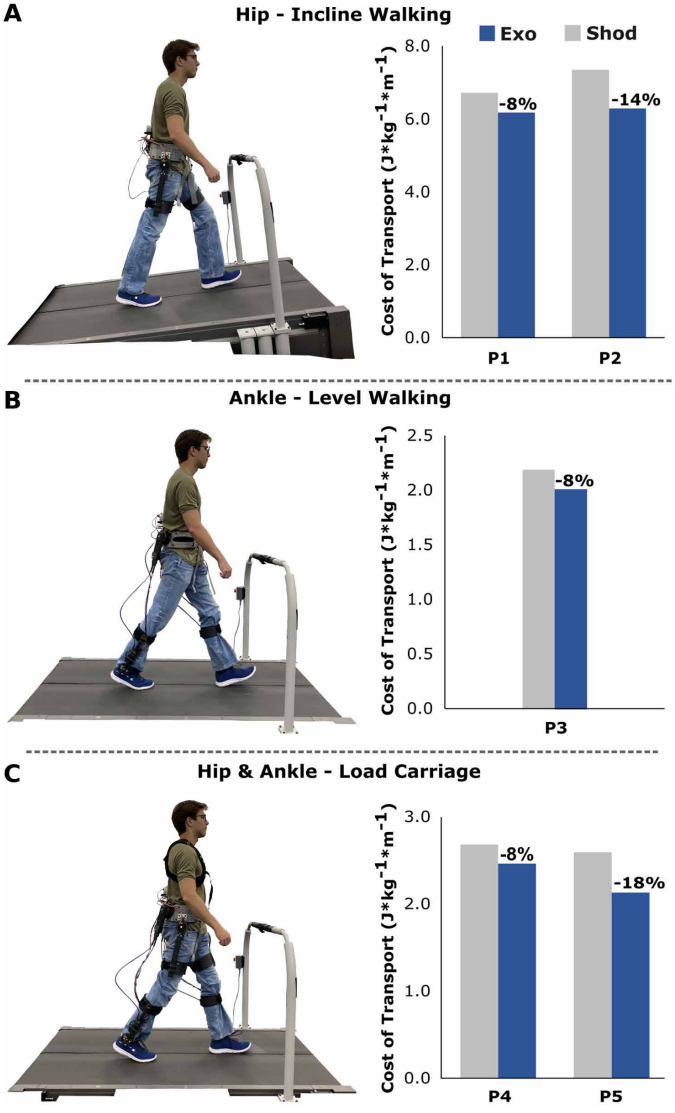

Fig. 4. COT for each of the experimental treadmill tasks. COT with and without (**A**) hip assistance during 7.5° incline walking ($n = 2$), (**B**) ankle assistance during level walking ($n = 1$), and (**C**) combined hip-and-ankle assistance while walking with a weighted vest ($n = 2$). Each user had a lower COT while receiving assistance (blue) when compared with walking without the device (gray). All three images are representative images of a user walking with the specified configuration during the task of interest.

with and without the device configured for ankle assistance in a 1650-m loop at a park (Fig. 5). The time to complete the loop and the number of steps taken with the right leg were recorded and used to calculate the average speed and stride length of the user. When walking outdoors in the exoskeleton (versus without), the user completed the loop faster and with fewer steps, resulting in a longer average stride length and a faster average walking speed (Fig. 5C), suggesting improved mobility while using the device.

Elbow assistance during weightlifting

Surface electromyography (EMG) electrodes were placed on the short head of the biceps brachii of the dominant arm of two individuals (P6 and P7; table S1). These individuals then performed weight curls with a 19.5-kg object until reaching fatigue with and without the device configured for elbow flexion assistance while we recorded muscle activity. A 60-beats-per-minute metronome prompted users to raise and lower the object (leading to a full cycle every 2 s) with a repetition being considered one complete cycle from the down position back to the down position (Fig. 6A). Both participants saw increases in the number of repetitions they could perform with elbow assistance (Fig. 6B). P6 increased their repetitions from 7 to 14 with assistance (+100%), whereas P7 increased their repetitions from 6 to 22 (+267%). These increased repetitions were supported by reductions in peak biceps activity (P6: −35%; P7: −57%). Together, these results indicate that elbow assistance during weightlifting may increase endurance of the user, which could lead to increased productivity and/or decreased injury risk in a physically demanding environment. More extensive testing ($n = 9$) with this configuration supported these findings, with other users demonstrating reduced fatigue during lifting and during more complex tasks in a simulated workplace environment (*26*).

DISCUSSION

This article describes the design and validation of an open-source exoskeleton system aimed at growing the field of wearable robotics. This tool can be used as presented or as a starting point to be modified for the user's own interests. Here, we outlined the design of the system's components, including the software, electronics, and multiple hardware configurations, and evaluated the device's function under these configurations.

The most important feature of the system is its modularity. In particular, the fully open-source and modular software system provides users access to a subcomponent of exoskeletons that is typically not accessible/detailed. The creation of a software structure, particularly one that is adaptable, is a time-consuming process that requires substantial troubleshooting and revision before productive research can be performed. For groups who have iterated on years of prior closed-source work, this is not much of a barrier, but for those looking to get started in the field and those without extensive expertise, the design of this subcomponent can be a daunting challenge that ultimately delays or prevents many from contributing to the field. Our hope is that those interested in pursuing exoskeleton research can use this software, and the other tools that are a part of this system, to begin exploring new and unique applications of these devices. Simultaneously, we hope that others who do have experience with exoskeletons can use this as an untethered test bed to begin to explore hardware and control approaches that take these devices outside of the laboratory setting. Our long-term vision for OpenExo is for researchers within and across disciplines to contribute to its growth by sharing their hardware and control approaches for all to access, ultimately accelerating the growth of the field, enhancing reproducibility, and moving us closer to a wearable future.

When evaluating OpenExo under its different configurations, we found fast and accurate responses. Under experimentally relevant step responses, the hip configuration had a rise time of 3 ms, and the ankle configuration had a rise time of 65 ms. These responses are comparable to those of other devices in the community, where rise times range from 14 to 32 ms for the hip (*33*–*35*) and 10 to 67 ms for the ankle (*36*–*38*). When walking with their designated controllers, both configurations were able to accurately track the prescribed torques, with RMSEs of ~7%. These accuracies align with those in

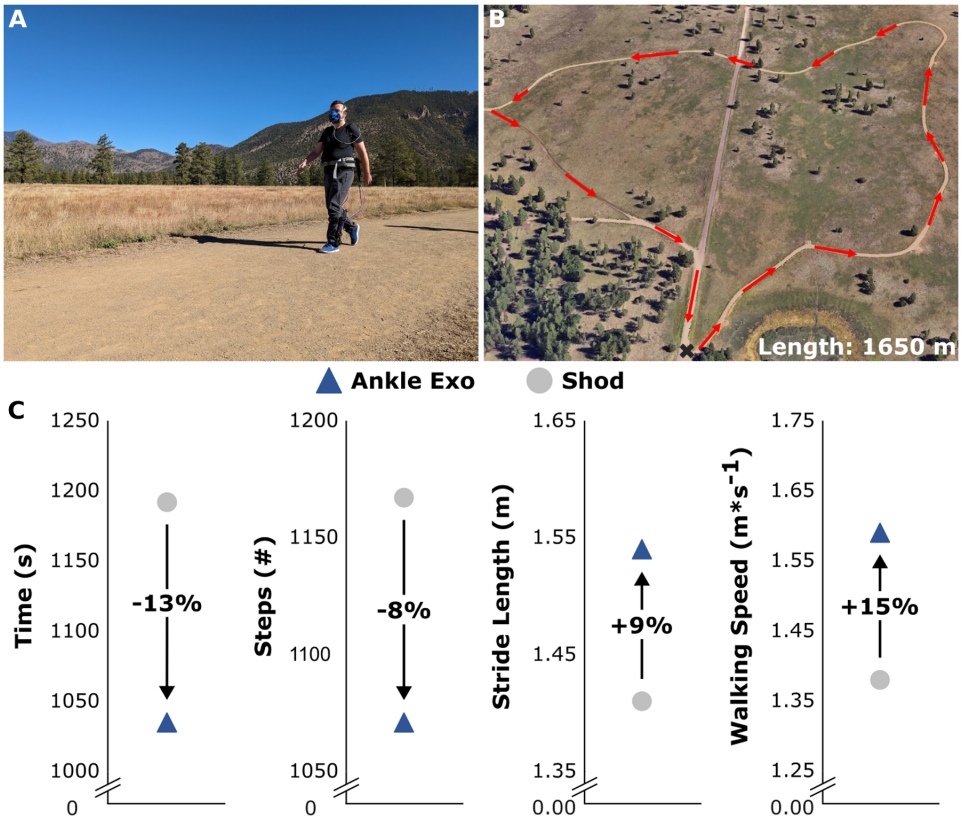

Fig. 5. Ankle exoskeleton assistance increased mobility while walking in a real-world setting (*n* = 1). (**A**) Participant walking around the outdoor course while receiving ankle exoskeleton assistance. (**B**) Outline of the outdoor course. (**C**) Experimental outcomes included course completion time, number of steps taken with the right leg, average stride length, and average walking speed with (blue triangles) and without (gray circles) ankle exoskeleton assistance. The participant completed the loop in a shorter time by walking with a longer stride and faster walking speed while receiving ankle assistance.

literature, which range from ~6 to 9% for both hip (*27*, *39*) and ankle devices (*27*, *30*). Although the performance of these configurations is comparable to that of others, it should be noted that differences in testing procedures make device-to-device comparison a challenge. Unlike the lower-extremity joints, we were unable to find any powered elbow devices to compare mechanical performance. Our hope is that the promising results from this study will serve as a basis to increase interest in this joint.

We evaluated the life span of each configuration when operating on a 22.2-V, 1800-mAh LiPo battery. The hip, ankle, and hip-and-ankle configurations were able to operate for 35, 25, and 15 min, respectively, before reaching 50% of the voltage capacity of the battery (~900 mAh). Similarly, the elbow configuration used 21% of its capacity after 30 min (122 cycles in the simulated workplace environment) and is projected to be able to operate for ~72 min before reaching the battery's 50% threshold. Operational life spans of exoskeletons are rarely reported in literature, likely because life span is dependent on the power source, hardware, control approach, and task. Although there are numerous factors that could influence this measure, we thought it important to characterize this aspect of performance to better understand the limiting factors for this open-source system when configured to our baseline recommendations. The universal limiting factor for each configuration, under the recommended settings, was battery life. The use of batteries with greater capacity may increase the operational life span of these devices but may come at the cost of added weight. In addition to battery voltage, we also examined motor temperatures. With the current operating durations, temperature was never a limiting factor; however, this may not hold true with larger-capacity batteries. Motor temperatures for some joints/configurations exceeded the American Society for Testing and Materials' temperature safety recommendations (C 1055-99), which note that 5 s of contact with temperatures greater than 60°C can lead to epidermal injury. To reduce risk of injury, we have designed heat shielding for each motor and transmission configuration (fig. S9).

We tested the capabilities of the device across multiple different hardware configurations. When configured for open-loop, direct-drive hip assistance, individuals exhibited metabolic improvements when walking on a 7.5° incline. These reductions in COT are consistent with prior work, which suggests that benefits could range from ~10 to 15% while receiving hip assistance on an inclined surface (*39*, *40*). Similar metabolic benefits have been found with hip assistance during level ground-walking (*28*, *41*–*43*), running (*44*), and stair-climbing (*45*) activities. When walking indoors with ankle plantar flexion assistance, we observed metabolic responses comparable to what others have found across a variety of tasks and populations (*28*, *29*, *46*–*48*). Although the metabolic benefits across these configurations are similar, the design and control approaches to achieve these benefits vary widely, limiting our understanding of what contributes to these responses. Future work by the community needs to refine our knowledge by isolating the design and control approaches that best improve performance under these configurations. During simultaneous assistance of the hips and ankles while users carried 22.2% of their body weight in additional load, we observed 8 and 18% reductions in the COT. Few have examined multijoint assistance because these devices typically incur a large mass penalty because of the hardware needed to achieve this type of assistance. Those who have investigated multijoint devices have overcome this challenge by using tethered systems that offload a substantial portion of the mass, at the cost of being confined to the laboratory (*27*, *28*), or by exploring different hardware approaches, such as soft exoskeletons (*49*, *50*) and/or combined passive and active systems (*51*). Preliminary work in the multijoint domain suggests that multijoint devices may be able to far exceed the capabilities of single-joint devices, with some finding that combined hip-knee-and-ankle assistance could reduce a user's COT by upward of 50% (*28*). The continued development of efficient hardware and control approaches for multijoint devices is a key future direction for the field.

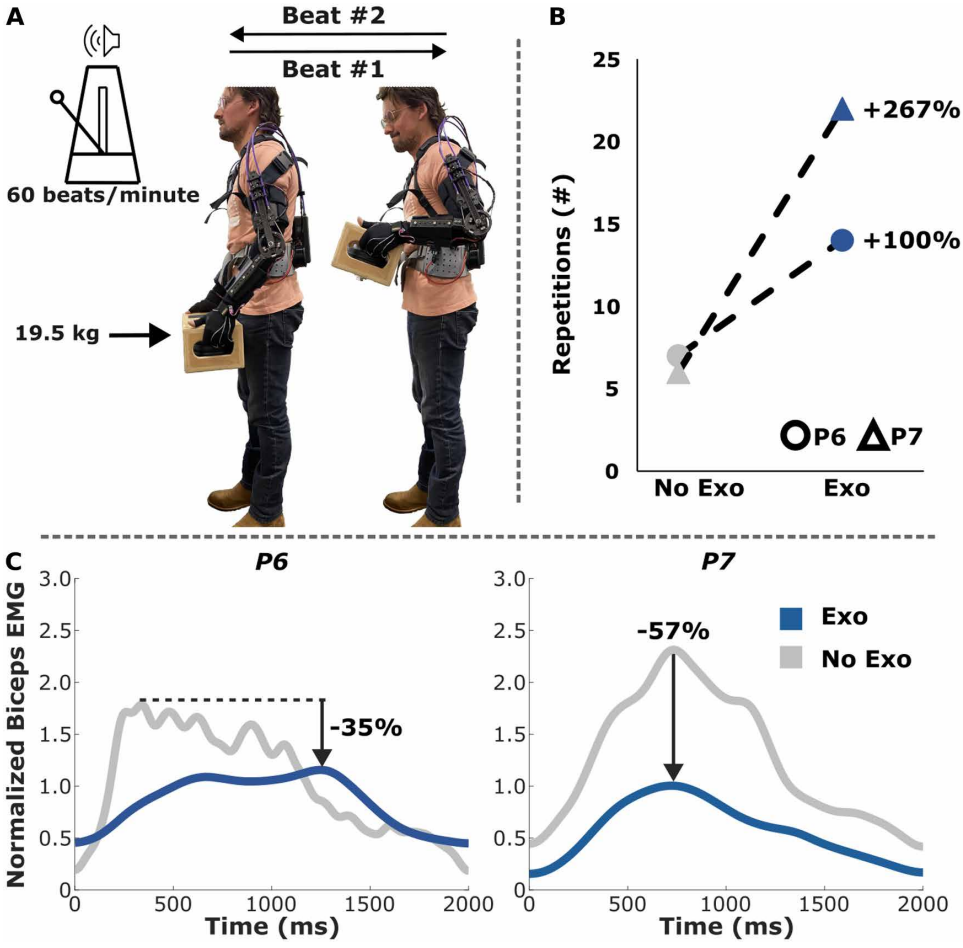

Fig. 6. Elbow assistance during weighted lifting resulted in decreased fatigue in users (n = 2). (**A**) Experimental protocol. Two users lifted a 19.5-kg box in time with a metronome while EMG activity was recorded from the short head of the biceps brachii of their dominant arm. (**B**) The number of repetitions increased by at least 100% for both users when receiving elbow assistance (blue) compared with not wearing the device (gray). (**C**) Similarly, decreases in peak bicep EMGs were detected with elbow joint assistance.

We had one user receive ankle assistance while on outdoor terrain and found that they had improved mobility, walking faster (+15%) with longer strides (+9%), compared with walking without the device. Most research with exoskeletons is performed in laboratory settings because it is easier to minimize confounding variables in these environments. Although laboratory tests are valuable to understanding the potential of exoskeletons, more work must be done when using these devices in their intended settings. These include outdoor, clinical, and at-home environments where challenges like mixed terrains and surfaces, differences in gait mechanics, and variable walking speeds may dampen the utility of laboratory-based findings. For example, the user in this study reported decreased stability and comfort with exoskeleton assistance because the application of power while walking on a dirt pathway seemed to alter the traction between the user's feet and the ground. Although only the report of one individual's experience, this interaction would not have been detected in a laboratory environment, and thus a potential insight into how these devices interact with their users would have been missed. Others have begun exploring the potential for translating exoskeletons beyond the laboratory, reporting mixed results. Using an ankle exoskeleton with human-in-the-loop informed control parameters, Slade *et al.* (*12*) found that users walked 9% faster while reducing the energy used to travel a given distance by 17% compared with walking without the device in an outdoor environment. Tagoe *et al.* (*13*) found that ankle assistance led to metabolic improvements when assisting those with cerebral palsy on a mixed-terrain outdoor course. In contrast, MacLean and Ferris (*52*), who examined knee assistance during loaded incline walking in the laboratory and in mixed-terrain outdoor settings, only saw a benefit of assistance indoors. It is evident that outdoor environments present substantial challenges to evaluating the viability of devices and control strategies when compared with the laboratory. One reason for this could be the field's reliance on metabolic measurements as a means for verifying device utility. This measurement is highly variable and thus necessitates steady-state tasks to have a degree of validity. Unfortunately, mixed-terrain, real-world settings are often not conducive to steady-state tasks and thus make user's energetics a poor measure in these domains. Future work aimed at identifying new ways to evaluate device efficacy is paramount for the field to expand into the real world.

Unlike lower-extremity devices that have struggled to move beyond the laboratory, upper extremity devices have had more success given their task-oriented nature (*53*, *54*). In this study, we outlined an elbow exoskeleton operating on this open-source infrastructure. Using this configuration, we found that two users were able to increase the number of weightlifting repetitions (+100 and +267%) while seeing corresponding reductions in biceps muscle activity (−35 and −57%). A full breakdown of this device, its control paradigm, and its utility during realistic labor tasks can be found in (*26*). Previous work exploring other upper extremity targets like the shoulder and back has demonstrated benefits that could be applicable in ergonomic settings (*15*, *18*, *55*, *56*). The elbow joint has been targeted less often (*54*), with only a handful of previous studies having explored untethered devices, with most being passive in nature (*57*). These previous attempts at assisting this joint have lacked autonomous usability and have generally only been tested during static tasks (*33*, *58*–*60*). The elbow configuration developed on this system is among the first to provide fully autonomous usage while also enabling dynamic work to be performed. Few have explored the utility of combining upper and lower extremity systems, despite their obvious ergonomic potential. Future work exploring this domain and its uses for real-world applications may be the shortest route to integrating exoskeletons into our everyday lives.

There are several promising future directions for OpenExo. First, we will continue to update our documentation for the system as we

develop new components and receive feedback from the community. Second, the system is now limited by its battery life (a common challenge with untethered systems), especially during high-torque multijoint applications. We will continue to explore potential solutions to increase operational duration. Third, we will continue to update and optimize the companion Python application available to users to help control the device. To date, it has several features, such as the ability to plot, record, and store data; update controllers and parameters in real time; and provide biofeedback (*61*). Further expanding this application to include state-of-the-art research capabilities, like deep learning (*62*) and human-in-the-loop approaches (*48*), is a high priority. Last, the experimental validation of the configurations presented in this paper was limited by the lack of more comprehensive analyses, such as the biomechanical consequences of each configuration, and small sample sizes. Although more biomechanically in-depth analyses and larger sample sizes would increase confidence in the findings, our primary goal was to highlight the modularity of the system and provide examples of its possible benefits during typical research tasks. Nonetheless, the experimental results of this paper should be interpreted with caution because the metabolic focus and small sample sizes likely do not capture the average person's response to these devices. Given these limitations, we would like to emphasize that the findings demonstrated here are solely intended to show that benefits with device usage may be possible and should not necessarily be expected in studies with larger sample sizes. Given the open-source nature of the device, we believe that it represents a promising solution to rectify the small–sample size nature of most exoskeleton studies. Specifically, this system could enable increased collaboration and large multisite studies exploring applications of exoskeletons, something that has previously evaded the community.

In summary, we believe that OpenExo will facilitate future directions for the field. Several excellent reviews have summarized the current state of research related to wearable robotics (*6*, *63*, *64*). This includes work on tethered systems and their use as laboratory-based test beds to explore control schemes (*27*, *28*), the combination of passive and active designs to enhance the ability and life span of devices (*36*, *51*, *65*), and understanding how individuals acclimate (*66*) and respond to devices (*67*). There has also been a large push by the field to incorporate aspects of machine learning and artificial intelligence to expand the capabilities of these devices (*68*). Critical future developments include the continued expansion of exoskeleton usage beyond the laboratory, including hybrid devices designed to assist or rehabilitate individuals with impairments or injuries in clinical and at-home environments (*69*) and the development of new methods to evaluate these devices, how they affect us, and how they can best serve us in society. Our hope is that OpenExo will present opportunities for those with valuable expertise outside the domain of exoskeletons to lend their experiences to help advance some of these research directions. For example, computer scientists who may lack the technical expertise needed to design and construct systems but who have expert knowledge in emerging domains like artificial intelligence may be able to incorporate their knowledge and make contributions to developing highly adaptable exoskeletons capable of usage in any setting. This could also include experts in domains like materials science, renewable energy and smart batteries, thermo-fluid systems, actuator development, fashion/clothing design, and medicine. In addition, we hope that researchers using this platform will share their own innovative designs, controllers, and assessment approaches, given that advancing research necessitates a team effort. As we continue to develop and expand this system, we will also continue to develop theopenexo.org to help serve as a centralized location for all to share their work. Last, we hope that this system will serve as a valuable educational tool for anyone interested in this field, because the continued inspiration and education of new researchers is a key building block in the development of fully realized devices that can change the lives of those in need.

MATERIALS AND METHODS

OpenExo consists of four subsystems: software, electronics, hardware, and controls. Each of these will be detailed independently, but for the sake of brevity, we will only highlight the open-source designs in this section. Information on the software, electronics, and controls, as well as the methodology for the benchtop and experimental validation, can be found in the Supplementary Materials.

Exoskeleton design

Waist belt

The waist belt is the core connection between the user and the robotic hardware. Thus, finding a comfortable belt that can accommodate multiple motors at a time (up to four) was a priority. We settled on an adjustable hip belt used for outdoor recreational activities (Osprey IsoForm 4), which has adequate padding for comfort. Four sizes (extra small, small, medium, and large) were used to provide flexibility to conform to the wearer. Each belt was modified by attaching a custom-designed 3D-printed assembly containing the PCB and battery (fig. S5). A 22.2-V, 1800-mAh LiPo battery was used throughout the study.

Hip device

We designed a bilateral, direct-drive untethered hip configuration capable of providing flexion and extension assistance (fig. S3A). The main design goals were to create a lightweight device that was simple to construct, could provide relevant magnitudes of assistance, was low cost, and could adjust to a broad range of anatomical geometries. To accomplish this, the waist belt assembly was modified to allow for the placement of motors in line with the hip-joint center. Our design consisted of three main components: the modified waist belt, the belt-motor connection, and the motor-thigh assembly. The waist belt was modified by adding mounting plates on each side of the belt in line with the hips. A grid of M5 clearance holes was drilled into the mounting plates to allow for flexibility in placement of the belt-motor connection to account for anatomical variability from person to person. The belt-motor connection consisted of an aluminum abduction/adduction hinge capable of facilitating out-of-plane motion during walking and carbon fiber brackets to interface the motor with the hinge. We used AK60-6v1.1 motors (CubeMars; Nanchang, Jiangxi, China), which were selected because of the relatively lower torques required of hip assistance (compared with the ankle joint) and their lower mass compared with more powerful alternatives (AK80-9). These motors were connected to a carbon fiber upright parallel to the user's leg via a custom-designed interface consisting of carbon fiber and 3D-printed onyx materials (carbon-reinforced nylon; fig. S3A). This interface directly connects to the carbon fiber upright, causing the upright to actuate with the motor. Thigh cuffs were designed to slide onto the upright to help facilitate torque transmission from the motor-upright configuration to the user. These cuffs were designed to conform to the shape of an individual's leg, were outfitted with padding to provide comfort, and

included an adjustable strap mechanism. Different sizes were designed to allow easy swapping to match user size.

Interfacing with the hardware located at the hips and thighs are bilateral heel and toe FSRs placed underneath the insoles of the wearer's shoes. These measure the relative force placed on each aspect of the foot and allow for control paradigms based on estimates of heel and toe contact with the ground, such as gait-phase–based control schemes. The total mass of this configuration is 2.9 kg.

Ankle device

The ankle-assembly end effector is nearly identical to our previous design (*29*) and is further detailed in the Supplementary Methods. Here, we highlight the open-source waist-mounted Bowden-cable transmission system (fig. S4). The 3D-printed motor-belt interfaces were designed to attach the motors to the waist belt (fig. S3B). All motors were placed outside the electrical casing to facilitate rapid swapping of device configurations. To further enhance modularity, these interfaces were designed for multiple versions of the AK series motors (AK80-9, AK60-6v1.1, and AK70-10). For the sake of brevity and clarity, all references to the ankle device will be to its AK80-9 configuration. A custom-designed 26-mm sprocket was fastened onto each motor to turn chains within a 3D-printed cartridge. Steel cables interfaced with the chains via custom-designed aluminum interfaces and were passed through Bowden sheaths to guide them to the ankle end-effector assembly. At the bottom of the 3D-printed cartridge, we designed a strain-relief system to minimize high strains where the Bowden sheathes exit the cartridge. This system consisted of a 3D-printed onyx casing that interfaced with 3D-printed thermoplastic polyurethane inserts that housed the Bowden sheaths. Some activities require high torque demands that may place more load on the steel cables than is recommended for the system; details on larger-diameter cables for high-torque (>30 Nm) activities are available in our hardware documentation.

The total mass of the ankle configuration, when sized to a 6-foot (182.88-cm)-tall adult, is 3.9 kg. This likely represents the largest weight for the system, given that the motors (and the associated cartridges), cable transmission system (length of steel cables and Bowden tubes), and the custom-designed footplates and calf cuffs were all at their largest.

Elbow device

To demonstrate the flexibility of the designed open-source framework, we also developed a bilateral, sagittal plane, elbow exoskeleton (fig. S2D) (*26*). A full description of the hardware and controls for this configuration is outlined in (*26*); here, we provide a general overview. Briefly, using a similar Bowden-cable driven transmission as the one used for our ankle exoskeleton device, motors (AK60-6v1.1s) mounted at the waist actuated steel cables that rotated a pulley placed in line with the elbow joint. This system interfaced with the user via custom-designed carbon fiber uprights and 3D-printed forearm and upper-arm cuffs as well as an upper-torso harness. The cuffs, harness, and waist belt were all adjustable to fit a variety of users. To facilitate low-level control schemes, a torque transducer was placed in line with the pulley and elbow to estimate sagittal plane elbow moments. To facilitate high-level control, small FSRs were placed on each hand at the proximal phalanges of the middle, ring, and little fingers (wired in parallel to create a single FSR signal) and on the palm at the base of the thumb. The device operated at zero torque (only applying torque to offset the resistance of the cable-driven system) when the FSR value was below a user-defined threshold and provided flexion assistance when it exceeded this threshold. A low-level proportional-derivative controller was used to perform closed-loop control to ensure the prescribed torques matched those measured from the torque transducer.

Experimental validation

To demonstrate the versatility and utility of our open-source system, we recruited healthy adults ($n = 7$; table S1) to complete activities while the device operated in different configurations. Inclusion criteria included age between 10 and 65 years, no lower-extremity orthopedic surgery within the prior 6 months, and no other health condition that would prevent safe completion of the protocol. Before enrollment, all participants granted written informed consent of an Institutional Review Board–approved protocol. In addition, all individuals depicted in this work consented to having their pictures published.

Statistical analysis

Given the small sample sizes for each experimental configuration, no statistical analyses were performed. All variables of interest were compared between the shod and exoskeleton conditions by calculating percent change, defined as

$$\%\,\text{Change} = \frac{\text{Exo} - \text{Shod}}{\text{Shod}} * 100 \quad (1)$$

Supplementary Materials

The PDF file includes:
Materials and Methods
Figs. S1 to S12
Table S1

Other Supplementary Material for this manuscript includes the following:
MDAR Reproducibility Checklist

REFERENCES AND NOTES

1. G. S. Sawicki, O. N. Beck, I. Kang, A. J. Young, The exoskeleton expansion: Improving walking and running economy. *J. Neuroeng. Rehabil.* **17**, 1–9 (2020).
2. Y. Fang, G. Orekhov, Z. F. Lerner, Improving the energy cost of incline walking and stair ascent with ankle exoskeleton assistance in cerebral palsy. *IEEE Trans. Biomed. Eng.* **69**, 2143–2152 (2022).
3. G. Orekhov, Y. Fang, J. Luque, Z. F. Lerner, Ankle exoskeleton assistance can improve over-ground walking economy in individuals with cerebral palsy. *IEEE Trans. Neural Syst. Rehabil. Eng.* **28**, 461–467 (2020).
4. K. Harshe, E. Tagoe, C. Bowersock, Z. F. Lerner, Priming robotic plantarflexor resistance with assistance to improve ankle power during exoskeleton gait training. *IEEE Robot. Autom. Lett.* **9**, 10511–10518 (2024).
5. J. S. Lora-Millan, F. J. Sanchez-Cuesta, J. P. Romero, J. C. Moreno, E. Rocon, Robotic exoskeleton embodiment in post-stroke hemiparetic patients: An experimental study about the integration of the assistance provided by the REFLEX knee exoskeleton. *Sci. Rep.* **13**, 1–16 (2023).
6. C. Siviy, L. M. Baker, B. T. Quinlivan, F. Porciuncula, K. Swaminathan, L. N. Awad, C. J. Walsh, Opportunities and challenges in the development of exoskeletons for locomotor assistance. *Nat. Biomed. Eng.* **7**, 456–472 (2023).
7. A. Nilsson, K. S. Vreede, V. Häglund, H. Kawamoto, Y. Sankai, J. Borg, Gait training early after stroke with a new exoskeleton - The hybrid assistive limb: A study of safety and feasibility. *J. Neuroeng. Rehabil.* **11**, 1–10 (2014).
8. D. R. Louie, J. J. Eng, Powered robotic exoskeletons in post-stroke rehabilitation of gait: A scoping review. *J. Neuroeng. Rehabil.* **13**, 1–10 (2016).
9. Y. Fang, K. Harshe, J. R. Franz, Z. F. Lerner, Feasibility evaluation of a dual-mode ankle exoskeleton to assist and restore community ambulation in older adults. *Wearable Technol.* **3**, 1–13 (2022).
10. E. Martini, S. Crea, A. Parri, L. Bastiani, U. Faraguna, Z. McKinney, R. Molino-Lova, L. Pratali, N. Vitiello, Gait training using a robotic hip exoskeleton improves metabolic gait efficiency in the elderly. *Sci. Rep.* **9**, 1–12 (2019).
11. H. J. Lee, S. Lee, W. H. Chang, K. Seo, Y. Shim, B. O. Choi, G. H. Ryu, Y. H. Kim, A wearable hip assist robot can improve gait function and cardiopulmonary metabolic efficiency in elderly adults. *IEEE Trans. Neural Syst. Rehabil. Eng.* **25**, 1549–1557 (2017).
12. P. Slade, M. J. Kochenderfer, S. L. Delp, S. H. Collins, Personalizing exoskeleton assistance while walking in the real world. *Nature* **610**, 277–282 (2022).

13. E. A. Tagoe, Y. Fang, J. R. Williams, Z. F. Lerner, Walking on real-world terrain with an ankle exoskeleton in cerebral palsy. *IEEE Trans. Med. Robot. Bionics* **6**, 202–212 (2024).
14. W. Huo, S. Mohammed, Y. Amirat, K. Kong, Fast gait mode detection and assistive torque control of an exoskeletal robotic orthosis for walking assistance. *IEEE Trans. Robot.* **34**, 1035–1052 (2018).
15. P. R. Slaughter, K. M. Rodzak, S. J. Fine, C. C. Ice, D. N. Wolf, K. E. Zelik, Evaluation of US Army soldiers wearing a back exosuit during a field training exercise. *Wearable Technol.* **4**, e20 (2023).
16. K. L. Mudie, A. C. Boynton, T. Karakolis, M. P. O'Donovan, G. B. Kanagaki, H. P. Crowell, R. K. Begg, M. E. LaFiandra, D. C. Billing, Consensus paper on testing and evaluation of military exoskeletons for the dismounted combatant. *J. Sci. Med. Sport* **21**, 1154–1161 (2018).
17. L. Van Engelhoven, N. Poon, H. Kazerooni, A. Ban, D. Rempel, C. Harris-Adamson, Evaluation of an adjustable support shoulder exoskeleton on static and dynamic overhead tasks. *Proc. Human Factors Ergonomics Soc.* **2**, 804–808 (2018).
18. E. P. Lamers, J. C. Soltys, K. L. Scherpereel, A. J. Yang, K. E. Zelik, Low-profile elastic exosuit reduces back muscle fatigue. *Sci. Rep.* **10**, 1–16 (2020).
19. O. Flor-Unda, B. Casa, M. Fuentes, S. Solorzano, F. Narvaez-Espinoza, P. Acosta-Vargas, Exoskeletons: Contribution to occupational health and safety. *Bioengineering* **10**, 1–24 (2023).
20. M. Bake, Is there a reproducibility crisis in science? *Nature* **533**, 452–454 (2016).
21. A. F. Azocar, L. M. Mooney, J. F. Duval, A. M. Simon, L. J. Hargrove, E. J. Rouse, Design and clinical implementation of an open-source bionic leg. *Nat. Biomed. Eng.* **4**, 941–953 (2020).
22. P. Foehn, E. Kaufmann, A. Romero, R. Penicka, S. Sun, L. Bauersfeld, T. Laengle, G. Cioffi, Y. Song, A. Loquercio, D. Scaramuzza, Agilicious: Open-source and open-hardware agile quadrotor for vision-based flight. *Sci. Robot.* **7**, 1–14 (2022).
23. A. G. Zisimatos, M. V Liarokapis, C. I. Mavrogiannis, K. J. Kyriakopoulos, "Open-source, affordable, modular, light-weight, underactuated robot hands" in *IEEE/RSJ International Conference on Intelligent Robots and Systems* (IEEE, 2014), pp. 1–6.
24. J. F. Duval, H. M. Herr, "FlexSEA: Flexible, Scalable Electronics Architecture for wearable robotic applications" in *Proceedings of the IEEE RAS and EMBS International Conference on Biomedical Robotics and Biomechatronics* (IEEE, 2016), pp. 1236–1241.
25. M. Cardona, C. E. García Cena, F. Serrano, R. Saltaren, ALICE: Conceptual development of a lower limb exoskeleton robot driven by an on-board musculoskeletal simulator. *Sensors* **20**, 1–20 (2020).
26. D. Colley, C. D. Bowersock, Z. F. Lerner, A lightweight powered elbow exoskeleton for manual handling tasks. *IEEE Trans. Med. Robot. Bionics* **6**, 1627–1636 (2024).
27. G. M. Bryan, P. W. Franks, S. C. Klein, R. J. Peuchen, S. H. Collins, A hip–knee–ankle exoskeleton emulator for studying gait assistance. *Int. J. Rob. Res.* **40**, 722–746 (2021).
28. P. W. Franks, G. M. Bryan, R. M. Martin, R. Reyes, A. C. Lakmazaheri, S. H. Collins, Comparing optimized exoskeleton assistance of the hip, knee, and ankle in single and multi-joint configurations. *Wearable Technol.* **2**, e16 (2021).
29. G. Orekhov, Y. Fang, C. F. Cuddeback, Z. F. Lerner, Usability and performance validation of an ultra-lightweight and versatile untethered robotic ankle exoskeleton. *J. Neuroeng. Rehabil.* **18**, 1–16 (2021).
30. G. M. Gasparri, J. Luque, Z. F. Lerner, Proportional joint-moment control for instantaneously adaptive ankle exoskeleton assistance. *IEEE Trans. Neural Syst. Rehabil. Eng.* **27**, 751–759 (2019).
31. R. W. Nuckols, K. Z. Takahashi, D. J. Farris, S. Mizrachi, R. Riemer, G. S. Sawicki, Mechanics of walking and running up and downhill: A joint-level perspective to guide design of lower-limb exoskeletons. *PLOS ONE* **15**, 1–20 (2020).
32. J. Brockway, Derivation of formulae used to calculate energy expenditure in man. *Hum. Nutr. Clin. Nutr.* **41**, 463–471 (1987).
33. J. Nassour, G. Zhao, M. Grimmer, Soft pneumatic elbow exoskeleton reduces the muscle activity, metabolic cost and fatigue during holding and carrying of loads. *Sci. Rep.* **11**, 1–14 (2021).
34. M. K. Ishmael, D. Archangeli, T. Lenzi, A powered hip exoskeleton with high torque density for walking, running, and stair ascent. *IEEE/ASME Trans. Mechatron.* **27**, 4561–4572 (2022).
35. V. L. Chiu, M. Raitor, S. H. Collins, Design of a hip exoskeleton with actuation in frontal and sagittal planes. *IEEE Trans. Med. Robot. Bionics* **3**, 773–782 (2021).
36. G. Orekhov, Z. F. Lerner, Design and electromechanical performance evaluation of a powered parallel-elastic ankle exoskeleton. *IEEE Robot. Autom. Lett.* **7**, 8092–8099 (2022).
37. J. Chen, J. Han, J. Zhang, Design and evaluation of a mobile ankle exoskeleton with switchable actuation configurations. *IEEE/ASME Trans. Mechatronics* **27**, 1846–1853 (2022).
38. S. Zhao, K. Walters, J. M. Perez, R. D. Gregg, "Design and validation of a modular, backdrivable ankle exoskeleton" in *IEEE International Conference on Biomedical Robotics and Biomechatronics* (IEEE, 2024), pp. 1–4.
39. S. S. Pour Aji Bishe, L. Liebelt, Y. Fang, Z. F. Lerner, "A low-profile hip exoskeleton for pathological gait assistance: Design and pilot testing" in *Proceedings of the IEEE International Conference on Robotics and Automation* (IEEE, 2022), pp. 5461–5466.
40. K. Seo, J. Lee, Y. J. Park, "Autonomous hip exoskeleton saves metabolic cost of walking uphill" in *IEEE International Conference on Rehabilitation Robotics* (IEEE, 2017), pp. 246–251.
41. W. Cao, C. Chen, H. Hu, K. Fang, X. Wu, Effect of hip assistance modes on metabolic cost of walking with a soft exoskeleton. *IEEE Trans Autom Sci Eng* **18**, 426–436 (2021).
42. Y. Lee, S. G. Roh, M. Lee, B. Choi, J. Lee, J. Kim, H. Choi, Y. Shim, Y. J. Kim, "A flexible exoskeleton for hip assistance" in *Proceedings of the IEEE International Conference on Intelligent Robots and Systems* (2017), pp. 1058–1063.
43. K. Seo, J. Lee, Y. Lee, T. Ha, Y. Shim, "Fully autonomous hip exoskeleton saves metabolic cost of walking" in *Proceedings of the IEEE International Conference on Robotics and Automation* (IEEE, 2016), pp. 4628–4635.
44. J. Kim, R. Heimgartner, G. Lee, N. Karavas, D. Perry, D. L. Ryan, A. Eckert-Erdheim, P. Murphy, D. K. Choe, I. Galiana, C. J. Walsh, "Autonomous and portable soft exosuit for hip extension assistance with online walking and running detection algorithm" in *Proceedings of the IEEE International Conference on Robotics and Automation* (IEEE, 2018), pp. 5473–5480.
45. D. S. Kim, H. J. Lee, S. H. Lee, W. H. Chang, J. Jang, B. O. Choi, G. H. Ryu, Y. H. Kim, A wearable hip-assist robot reduces the cardiopulmonary metabolic energy expenditure during stair ascent in elderly adults: A pilot cross-sectional study. *BMC Geriatr.* **18**, 1–8 (2018).
46. L. M. Mooney, E. J. Rouse, H. M. Herr, Autonomous exoskeleton reduces metabolic cost of human walking during load carriage. *J. Neuroeng. Rehabil.* **11**, 1–11 (2014).
47. S. Galle, P. Malcolm, S. H. Collins, D. De Clercq, Reducing the metabolic cost of walking with an ankle exoskeleton: Interaction between actuation timing and power. *J. Neuroeng. Rehabil.* **14**, 1–16 (2017).
48. J. Zhang, P. Fiers, K. A. Witte, R. W. Jackson, K. L. Poggensee, C. G. Atkeson, S. H. Collins, Human-in-the-loop optimization of exoskeleton assistance during walking. *Science* **356**, 1280–1284 (2017).
49. W. Cao, C. Chen, D. Wang, X. Wu, L. Chen, T. Xu, J. Liu, A lower limb exoskeleton with rigid and soft structure for loaded walking assistance. *IEEE Robot. Autom. Lett.* **7**, 454–461 (2022).
50. F. A. Panizzolo, I. Galiana, A. T. Asbeck, C. Siviy, K. Schmidt, K. G. Holt, C. J. Walsh, A biologically-inspired multi-joint soft exosuit that can reduce the energy cost of loaded walking. *J. Neuroeng. Rehabil.* **13**, 1–13 (2016).
51. W. Cao, Z. Zhang, C. Chen, Y. He, D. Wang, X. Wu, Biomechanical and physiological evaluation of a multi-joint exoskeleton with active-passive assistance for walking. *Biosensors* **11**, 1–15 (2021).
52. M. K. MacLean, D. P. Ferris, Energetics of walking with a robotic knee exoskeleton. *J. Appl. Biomech.* **35**, 320–326 (2019).
53. T. Moeller, J. Krell-Roesch, A. Woll, T. Stein, Effects of upper-limb exoskeletons designed for use in the working environment—A literature review. *Front. Robot. AI* **9**, 1–15 (2022).
54. L. Botti, R. Melloni, Occupational exoskeletons: Understanding the impact on workers and suggesting guidelines for practitioners and future research needs. *Appl. Sci.* **14**, 1–28 (2024).
55. J. Chung, D. A. Quirk, M. Applegate, M. Rouleau, N. Degenhardt, I. Galiana, D. Dalton, L. N. Awad, C. J. Walsh, Lightweight active back exosuit reduces muscular effort during an hour-long order picking task. *Commun. Eng.* **3**, 1–11 (2024).
56. S. Ding, A. Reyes Francisco, T. Li, H. Yu, A novel passive shoulder exoskeleton for assisting overhead work. *Wearable Technol.* **4**, e7 (2023).
57. A. Winter, N. Mohajer, D. Nahavandi, "Semi-active assistive exoskeleton system for elbow joint" in *2021 IEEE International Conference on Systems, Man and Cybernetics* (IEEE, 2021), pp. 2347–2353.
58. Z. Yan, H. Yi, Z. Du, T. Huang, B. Han, L. Zhang, A. Peng, X. Wu, "Development of an assist upper limb exoskeleton for manual handling task" in *IEEE International Conference on Robotics and Biomimetics, ROBIO 2019* (IEEE, 2019), pp. 1815–1820.
59. J. L. Samper-Escudero, S. Coloma, M. A. Olivares-Mendez, M. A. S.-U. Gonzalez, M. Ferre, A compact and portable exoskeleton for shoulder and elbow assistance for workers and prospective use in space. *IEEE Trans. Human-Machine Syst.* **53**, 668–677 (2023).
60. F. Missiroli, N. Lotti, E. Tricomi, C. Bokranz, R. Alicea, M. Xiloyannis, J. Krzywinski, S. Crea, N. Vitiello, L. Masia, Rigid, soft, passive, and active: A hybrid occupational exoskeleton for bimanual multijoint assistance. *IEEE Robot. Autom. Lett.* **7**, 2557–2564 (2022).
61. B. C. Conner, Z. F. Lerner, "Improving ankle muscle recruitment via plantar pressure biofeedback during robot resisted gait training in cerebral palsy" in *IEEE International Conference on Rehabilitation Robotics* (IEEE, 2022), vol. 2022-July, pp. 25–29.
62. D. D. Molinaro, I. Kang, A. J. Young, Estimating human joint moments unifies exoskeleton control, reducing user effort. *Sci. Robot.* **9**, eadi8852 (2024).
63. A. J. Young, D. P. Ferris, State of the art and future directions for lower limb robotic exoskeletons. *IEEE Trans. Neural Syst. Rehabil. Eng.* **25**, 171–182 (2017).
64. X. Tang, X. Wang, X. Ji, Y. Zhou, J. Yang, Y. Wei, W. Zhang, A wearable lower limb exoskeleton: Reducing the energy cost of human movement. *Micromachines* **13**, 1–40 (2022).
65. E. Krimsky, S. H. Collins, Elastic energy-recycling actuators for efficient robots. *Sci. Robot.* **9**, eadj7246 (2024).

66. K. L. Poggensee, S. H. Collins, How adaptation, training, and customization contribute to benefits from exoskeleton assistance. *Sci. Robot.* **6**, eabf1078 (2021).
67. O. N. Beck, M. K. Shepherd, R. Rastogi, G. Martino, L. H. Ting, G. S. Sawicki, Exoskeletons need to react faster than physiological responses to improve standing balance. *Sci. Robot.* **8**, eadf1080 (2023).
68. D. D. Molinaro, K. L. Scherpereel, E. B. Schonhaut, G. Evangelopoulos, M. K. Shepherd, A. J. Young, Task-agnostic exoskeleton control via biological joint moment estimation. *Nature* **635**, 337–344 (2024).
69. C. D. Bowersock, Z. F. Lerner, Feasibility of using autonomous ankle exoskeletons to augment community walking in cerebral palsy. *IEEE Open J. Eng. Med. Biol.* **6**, 75–81 (2024).

Acknowledgments: We thank K. Harshe, P. Bosch, and C. Bowersock for assistance with some of the experimental data collection and L. Coonrod for assistance in developing and supporting documentation for the Python companion application. **Funding:** This work was supported in part by a Mary M. Winn-Radcliff and Gregory M. Winn Research Award (Z.F.L.), in part by the Eunice Kennedy Shriver National Institute of Child Health and Human Development of the National Institutes of Health under award number R01HD107277 (Z.F.L.), and in part by the National Science Foundation under grant number 2045966 (Z.F.L.). The content is solely the responsibility of the authors and does not necessarily represent the official views of the National Institutes of Health or the National Science Foundation. **Author contributions:** Conceptualization: J.R.W., C.F.C., P.P., and Z.F.L. Methodology: J.R.W., C.F.C., S.F., D.C., N.E., P.C., P.P., and Z.F.L. Investigation: J.R.W., C.F.C., S.F., D.C., N.E., P.C., P.P., and Z.F.L. Visualization: J.R.W., N.E., P.C., and Z.F.L. Funding acquisition: Z.F.L. Project administration: J.R.W. and Z.F.L. Supervision: J.R.W. and Z.F.L. Writing—original draft: J.R.W. Writing—review and editing: J.R.W., C.F.C., S.F., D.C., N.E., P.C., P.P., and Z.F.L. **Competing interests:** Z.F.L. is a cofounder with shareholder interest of Biomotum Inc., a university start-up company, seeking to commercialize exoskeleton technology. He also has intellectual property inventorship rights covering aspects of ankle exoskeleton design and control. Z.F.L. and D.C. are named inventors on US utility patent application number 19/196,598, titled "Lightweight powered elbow exoskeleton for manual handling tasks." **Data and materials availability:** All data, code, and materials used in the analysis are available for other researchers to use, replicate, and analyze. In addition, all material described above (software, electronics, and hardware) and their documentation (in their state at the time of publication) are included with this manuscript to further facilitate easy user access. The data and version of the OpenExo at the time of submission can be found at https://doi.org/10.5281/zenodo.14624972. Up-to-date versions of this material can be found on OpenExo's website (theopenexo.org).

Submitted 13 September 2024
Accepted 27 May 2025
Published 25 June 2025
10.1126/scirobotics.adt1591